Energy Management Policies for Passive RFID Sensors with RF-Energy Harvesting

Fabio Iannello*†, Osvaldo Simeone† and Umberto Spagnolini*
*DEI, Politecnico di Milano, Piazza Leonardo da Vinci 32, 20133 Milan, Italy
†CWCSPR, New Jersey Institute of Technology, University Heights, 07102 Newark, NJ, USA
Email: {fabio.iannello, osvaldo.simeone}@njit.edu, spagnoli@elet.polimi.it

***Abstract*— A critical performance criterion in backscatter modulation-based RFID sensor networks is the distance at which a RFID reader can reliably communicate with passive RFID sensors (or tags). This paper proposes to introduce a power amplifier (PA) and an energy storage device (such as a capacitor or a battery), in the hardware architecture of conventional passive RFID tags, with the aim of allowing amplification of the backscatter signal to increase the read range. This new tag architecture, referred to as Amplified Backscattering via Energy Harvesting (ABEH), can still be considered as passive, since the energy storage device is charged exclusively by harvesting energy from the RF-signal transmitted by the reader and received by the tag during idle periods. The harvested and stored energy is then used by the tags to opportunistically amplify the backscatter signal. It is noted that this architecture is significantly different from active RFID tags where the battery, charged at the time of installation, is used to supply a complete onboard transceiver so that no backscatter modulation is employed. Energy scheduling strategies, based on the trade-off between energy harvesting rate and successful transmission probability, are proposed. Performance analysis of tags with the proposed ABEH architecture is carried out over quasi-static fading channels by framing the design problem as a Markov Decision Process. Numerical results show remarkable improvement of the ABEH approach with respect to conventional passive RFID tags and provide insight into the effect of system parameters on the energy scheduling.**

I. Introduction

Passive Radio Frequency identification (RFID) technology is finding an ever increasing number of applications, ranging from conventional identification such as supply chain management or toll collections, to wireless sensor networks (WSN), where identification is provided along with sensed data [1]. A typical far-field passive RFID sensor network consists of one (or more) RFID reader and a number of RFID sensors (also tags in the sequel), where tags communicate data to the reader by modulating, possibly amplifying, and transmitting back a continuous wave (CW) emitted by the reader itself through a process called backscatter modulation [2].

The RF field emitted by the reader is the only source of energy that allows passive tags to activate their circuitries, while more sophisticated classes of tags, referred to as semi-active and active, rely on energy storage devices (simply batteries in the sequel) charged at the time of installation [2]. In semi-active tags the onboard battery is used to activate a part or all the tag circuitry, but the communication with the RFID reader is still performed through backscatter modulation as in passive tags (i.e., without the use of the on-board battery).

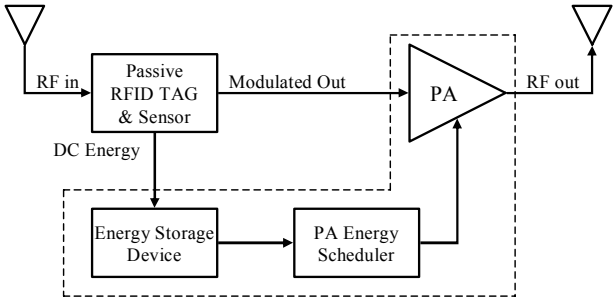

Fig. 1. Block diagram of an RFID ABEH sensor. The dashed box contains the novel components with respect to classic passive RFID sensors.

Active tags instead do not rely on backscatter modulation and use the battery to activate their circuitry including an on-board transceiver for communication with the reader. Active and semi-active tags enable more sophisticated applications at the price of increasing cost, and typically limited lifetime, with respect to passive tags.

One of the most important RFID system performance is the *read range*, or equivalently the maximum distance at which the reader can reliably read (or write) the RFID sensors [3]. Two main factors determine the read range: 1) *Tag sensitivity* (tag-limited regime), which is determined by the minimum power received by the tag necessary to activate its circuitry; 2) *Reader sensitivity* (reader-limited regime), which is determined by the minimum Signal to Noise Ratio (SNR), or alternatively the minimum power, at the reader that enables correct detection of the signal backscattered by the tag.

The new conceptual scheme that we propose in this paper aims to address the issue of reader-limited regime by introducing two additional components to the hardware architecture of conventional passive tags as shown in Fig. 1:

- A power amplifier (PA), which is used to amplify the backscatter signal (i.e., the reader's CW processed and transmitted back by the tag);
- An energy storage device (e.g., battery or capacitor), which is charged via energy harvesting.

This enhanced tag architecture, referred to as *Amplified Backscattering via Energy Harvesting* (*ABEH*), is still passive, in the sense that it does not need any initially charged battery (or capacitor): In fact, it exploits the RF-energy transmitted by the reader, and received by the tag during idle periods,

to recharge the onboard battery. The harvested energy is then used by the tags to opportunistically amplify the backscatter signal, with the goal to improve communication reliability. Notice that RFID tags with ABEH architecture (ABEH tags for short) inherit the theoretically infinite lifetime of passive tags, since in case of depleted battery they can operate as conventional passive tags.

An energy scheduler (not listed above as a new component, since it can be integrated in the control logic already present in the conventional passive architecture) manages the energy used by the PA to amplify the backscatter signal, by accounting for the current state of charge of the battery and the energy harvesting rate, in order to optimize the performance in terms of read range of ABEH tags. The analysis demonstrates that the amplification of the backscatter signal enhances the read range in the reader-limited regime of operation. It is noted that the analysis here could be extended to include the trade-off between energy used for backscatter amplification and for powering the tag circuitry (including the onboard sensor).

We now briefly review some prior work related to this paper. In [4] the problem of reader sensitivity is addressed in a similar fashion as ABEH tags by allowing amplified backscatter from the RFID tags. There, however, the PA is fed by an independent power source (active tags), thus differing from ABEH tags where the energy for amplification is harvested from the environment. The problem of tag-limited regime is addressed in [5], where an independent CW source is installed on the tag and acts as an energy pump fed by a battery, while in [6] sleep and wake cycles together with energy harvesting techniques are proposed. Transmission policies optimization for replenishable sensors is addressed in [7] where the authors resort to an analytical model based on Markov Decision Process (MDP). Battery-free RFID transponders with sensing capability that harvest all the needed energy from the RF signal emitted by the reader are investigated in [8, and references therein] together with possible applications. Discussion on energy storage architectures, for enhanced RFID tags, can be found in [9]. Measures and statistical characterization of the effect of the fading and path loss in a backscatter modulation-based system are presented in [10].

The paper is organized as follows. In Sec. II we introduce the signal and system models used throughout the paper, while Sec. III describes the working principle of ABEH tags. In Sec. IV we model the strictly interacting battery charging process and the energy scheduling as a MDP [11]. Numerical results are then presented in Sec. VI and finally some conclusions are drawn in Sec. VII together with future extensions.

II. System Model

We focus on a far-field RFID system, with a single-reader and multiple-tags [2][12]. The operation of the considered RFID network in the presence of passive tags can be generally summarized with the following phases (a commercial example is the Gen-2 standard [12]). The reader transmits a CW to energize the entire population of tags [6]. After a time period long enough for the tags to activate their circuitries

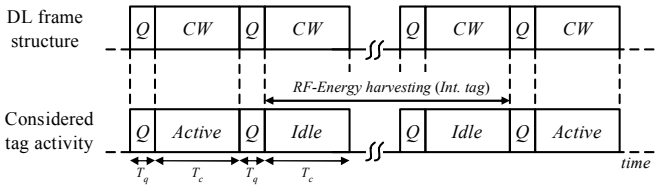

Fig. 2. Reader DL frame structure and interrogated tag activity. A single time-slot is composed by two parts: Query command (*Q*) and Continuous Wave (*CW*). During the CW period a tag can be either *active* (transmitting data) or *idle* (harvesting energy).

(by accumulating energy from the CW), the reader starts transmitting a modulated signal containing a selection command to choose a subset of tags. After this phase, the reader transmits sequence of *query* commands (Q) of T_q seconds each, to request information from the selected tags. Data transmission from the tags take place during a subsequent period of duration T_c, in which the selected tags perform backscatter modulation. The combination of a query command and CW forms a *time-slot* of duration $T = T_q + T_c$ (see Fig. 2).

A collision protocol is generally necessary to arbitrate the access of the (possibly multiple) selected tags. In order to simplify the problem and focusing on the energy management of ABEH tags, we assume here that in every time-slot one *single* tag is selected by the reader's query, independently from previous and future queries, to respond via backscatter modulation. Notice that the impact of collisions, due to the multiple access, could be taken into account by conveniently modifying the probability of successful transmission that will be defined in (7). However, this collision-free assumption is reasonable in scenarios where RFID tags are selected according to their unique identifiers (known at the reader) as possibly for RFID-based sensor networks (see [12]).

Because of both collision-free and independent queries assumptions, we can focus on a simplified single-reader single-tag scenario, where the downlink (DL) frame structure transmitted by the reader is composed by successive time-slots, each one containing a query command and CW as shown in Fig. 2. In each time-slot, the unique tag in this scenario (simply "the tag" in the sequel) after having decoded the query, can assume two different states (see Fig. 2):

- *Active time-slot* for the tag, with probability p it switches its state to active and performs backscatter modulation to transmit the required data to the reader (the tag is interrogated).
- *Idle time-slots* for the tag, with probability $1 - p$, it switches its state to idle and activates the RF-energy harvesting process (the tag is not interrogated).

Notice that in a general multiple-tags scenario, the interrogation probability p depends on the number of tags and on the rate at which the reader needs to collect information from each tag. Furthermore, the probability p can also take into account tag collisions at the reader and demodulation errors of the query commands (not explicitly modeled here).

We consider bistatic RFID readers that use two antennas,

one for transmission (TX antenna) and one for reception (RX antenna) (see [3] and [10]). We refer to the link TX antenna to tag and tag to RX antenna as downlink (DL) and uplink (UL) respectively. We assume the same distance d from tag to reader RX and TX antenna, which is also fixed for the entire operations. During time-slot k, the DL (UL) channel $h_{dl}(k)$ ($h_{ul}(k)$) is subject to fluctuations that are modeled as frequency-flat fading that are constant over the entire time-slot, while varying slot-by-slot as independent and identically distributed (i.i.d.) random variables. Assuming that the duration T_q of the query command is much shorter than the duration T_c of the CW (i.e., $T_q \ll T_c \simeq T$), the signal impinging on the tag is:

$$y(t;k) = \sqrt{L} h_{dl}(k) x(t) + w(t;k), \tag{1}$$

where $kT \leq t < (k+1)T$ runs over the k-th time-slot (of duration T), the energy per time-slot available for the transmission of the CW is E_0, the propagation loss between the reader and the tag is denoted by L and it is assumed constant as distance d is fixed, $x(t) = \sqrt{2E_0/T}\cos 2\pi f_0 t$ represents the CW transmitted by the reader of energy E_0, f_0 is the carrier frequency and $w(t;k)$ is an Additive White Noise (AWGN) in the band of interest characterized by $w(t;k) \sim \mathcal{N}(0, \sigma_t^2)$.

III. ABEH Functionality

ABEH tags are characterized by: 1) Harvesting and storing of energy during idle time-slots; 2) opportunistic amplification of the backscatter signal during active time-slots, as controlled by the energy scheduler. In principle, the energy $E_b(k)$ drawn from the battery by the energy scheduler in slot k may depend on a number of factors, such as the current state of charge of the battery $S(k)$, the energy evolution over the past time-slots, the interrogation probability p, the DL and UL channels quality (channel state information, CSI) and the path loss L. In practice, all this information cannot be dynamically tracked by simple devices like RFID tags and some simpler policies must be used. We consider scheduling policies (pre-determined and possibly stored into the tag memory) that do not depend on the entire history of previous observations, i.e., *stationary policies* (see, e.g., [11]). These policies depend on the following static system parameters, assumed to be time-invariant and known at the tag (or possibly communicated by the reader queries): interrogation probability p, path loss L and DL and UL channel statistics. The only quantity that needs to be measured by the tag is the *state* of the battery $S(k)$, i.e., the amount of energy currently stored.

Optimal policies need to balance the energy harvesting rate, which is out of the tag's control, and the probability of successful transmission, which can be controlled by the energy scheduler by varying the energy drawn from the battery for backscatter amplification. The goal of the energy scheduler is to maximize the performance (read range) of ABEH tags. We now characterize the harvesting process (idle time-slots) and then introduce the effects of the backscatter signal amplification on the backscatter SNR at the reader (active time-slots).

A. Idle Time-Slots: RF-Energy Harvesting

The energy received by the tag during time-slot k, can be easily derived from (1) as

$$E(k) = \int_{kT}^{(k+1)T} |y(t;k)|^2 \, dt \simeq L E_0 \, |h_{dl}(k)|^2 , \tag{2}$$

where the energy of the noise is negligible compared to signal energy: $L E_0 \, |h_{dl}(k)|^2 \gg \sigma_t^2 T$. In order to make the RF-energy available for storage, the signal (1) impinging on the tag passes through an RF-to-DC converter, with a conversion efficiency $\eta_{DC} \in [0,1)$ assumed as constant for all the RF input power levels (see [13] for a more detailed treatment). The energy available for storage during time-slot k is:

$$\mathcal{E}(k) = \eta_{DC} E(k) = \eta_{DC} L E_0 \, |h_{dl}(k)|^2 . \tag{3}$$

Notice that the randomness of the available energy $\mathcal{E}(k)$ is due to DL fading channel $|h_{dl}(k)|^2$ that might sum-up to the path-loss (not considered here as d is constant).

B. Active Time-Slots: Backscatter SNR

During active time-slots, the interrogated tag replies to reader queries by transmitting back information through backscatter modulation. With ABEH tags, the backscattered signals can be amplified by feeding the PA an amount of energy $E_b(k)$ from its on-board battery (see Sec. IV). The instantaneous SNR at the RFID reader during active time-slots can be written as (derivation is omitted here, see [3], [14]):

$$\gamma(E_b(k);k) = \frac{L^2 E_0 \, |h_{ul}(k)|^2 \, |h_{dl}(k)|^2}{\sigma_r^2 T} \eta_{\mathrm{mod}} + \frac{L \, |h_{ul}(k)|^2 \, E_b(k)}{\sigma_r^2 T} \eta_{amp}, \tag{4}$$

where σ_r^2 is the power of the AWGN at the reader, $h_{dl}(k)$ and $h_{ul}(k)$ are the DL and UL fading channels, respectively, $\eta_{\mathrm{mod}} \in [0,1)$ is the tag transmission efficiency accounting for the effects of the backscattering process [3], and $\eta_{amp} \in [0,1)$ is the efficiency of the PA. The first term in (4) is the SNR that we would have by using conventional passive tags that perform only backscatter modulation (see [10][14]). The second term is due to the amplification performed by the ABEH tag, and depends only on the UL channel.

IV. Battery Evolution: A Markov Chain Model

The evolution of the energy stored in the battery is modelled by resorting to a discrete Markov chain (e.g., [15]). The battery is of size $E_{\max}$ [J] and is uniformly divided into N states, representing different energy levels, where the *energy-unit*, is $\delta_E = E_{\max}/(N-1)$. The state of the battery is $S(k) \in \{0, ..., N-1\}$. It is noted that the discrete model at hand is an approximation of a continuous quantity (the harvested energy). Therefore, making δ_E as small as possible insures that the state of the battery can be modelled more accurately, but at the cost of increasing the complexity of the model.

We can define a stationary policy $\boldsymbol{\lambda} = [\lambda_0, ..., \lambda_{N-1}]^T$ as the set of actions that the energy scheduler takes for every possible value of the state variable $S(k)$ regardless of the time slot k, and fixed the system parameters as described in Sec. III. More specifically, action λ_n, for $n \in \{0, ..., N-1\}$, is a non-negative integer $\lambda_n \in \{0, ..., n\}$, corresponding to the number of energy-units δ_E (or equivalently $E_b(k) = \delta_E \lambda_n$) drawn from the battery for amplification when in state $S(k) = n$. Notice that, at state $S(k) = n$, the energy scheduler of the ABEH tag has $n + 1$ possible choices for λ_n, so that the total number of available stationary policies for N levels is $1 \cdot 2 \cdot ... \cdot N = N!$. The simplest policy that can be used as a reference is the *draw-all* policy, where all the energy currently stored in the battery is used to amplify the backscatter signal (i.e., $\lambda_n = n$). In the numerical results presented in Sec. VI we also consider strategies that are limited to schedule energy in steps larger than δ_E due to possible technological constraints.

A. Transition Probabilities

The evolution of the energy stored by the ABEH tag, depends on tag interrogation probability p, and channel properties. Specifically, energy harvesting during idle time-slots may determine transitions toward higher energy levels, depending on the channel quality (see Sec. III-A). Conversely, during active time-slots the energy scheduler draws some energy-units from the battery, thus determining a transition toward a lower energy level (see Sec. III-B).

For stationary energy scheduling policies, the state of the battery $S(k)$ evolves over the time-slots as an irreducible and aperiodic time-homogeneous Markov chain (see Fig. 3) (the Markov chain is thus ergodic). The transitions toward higher energy levels depend on the probability $q = 1-p$ of having an idle time-slot, and on the probability that the harvested energy $\mathcal{E}(k)$ (see (3)) allows the ABEH tag to store some energy-units δ_E. The conditional probability β_{nl} that, during an idle time-slot, there is a transition from state $S(k) = n$ to $S(k+1) = l$, can be obtained as follows:

$$\beta_{nl} = \Pr\left[S(k+1) = l | S(k) = n, idle\right] = \begin{cases} \Pr\left[(l-n)\delta_E \leq \mathcal{E}(k) < (l-n+1)\delta_E\right] & l \leq N-2 \\ \Pr\left[\mathcal{E}(k) \geq (l-n)\delta_E\right] & l = N-1 \\ 0 & 0 \leq l < n \end{cases}, \tag{5}$$

where the second row of the right-hand side of (5) accounts for the highest energy level, while the third row indicates that there is no energy leakage during idle time-slots. Notice that $\sum_{l=0}^{N-1} \beta_{nl} = 1$, for all $n \in \{0, ..., N-1\}$. Once again energy quantization δ_E should be small enough to capture small variation of the harvested energy $\mathcal{E}(k)$ when modelling the system. Conversely, during active time-slots the transition toward a lower, or at least the same, energy level, is deterministically defined by the policy $\boldsymbol{\lambda}$. To sum up, by resorting to the law of total probability, the n-th entry of the l-row $[\mathbf{P}]_{nl}$ of the transition probability matrix $\mathbf{P}$ for the Markov chain in Fig. 3 can be written as the sum of two contributions, one from idle-time slots with probability $(1-p)\beta_{nl}$, and one from active time-slots with probability p if and only if $\lambda_n = n - l$:

$$[\mathbf{P}]_{nl} = \Pr\left[S(k+1) = l | S(k) = n\right] = \begin{cases} (1-p)\beta_{nl} & l \neq n - \lambda_n \\ (1-p)\beta_{nl} + p & l = n - \lambda_n \end{cases}, \tag{6}$$

As we will see below, the problem of finding optimal stationary policies can be classified as a MDP.

V. Optimal Energy Scheduling

The aim of the ABEH tag is to improve the read range in the reader-limited regime (see Sec. I). Given the randomness induced by fading and noise at the reader, we evaluate the read range in terms of the probability that the reader correctly decodes the tag signal, referred to as read probability, for a given distance tag-reader. The read probability is defined as follows:

$$r(\lambda_n) = \Pr\left[\gamma(\lambda_n \delta_E; k) \geq \gamma_{th}\right], \tag{7}$$

where $\gamma(\lambda_n \delta_E; k)$ is the instantaneous SNR (see (4) with $E_b(k) = \lambda_n \delta_E$) at the reader given that ABEH tag battery is in state n and λ_n energy-units are drawn from the battery for backscatter amplification, while threshold γ_{th} is the minimum SNR that allows correct decoding. Notice that the dependence of the read probability (7) on the distance d, and thus the relation with the read range, is implicitly contained in the definition of the instantaneous SNR (4). In order to evaluate the average performance of the ABEH tag over an increasing number of active time-slots, we define the long-term average read probability as follows:

$$g(\boldsymbol{\lambda}) = \lim_{K \to \infty} \frac{1}{K} \sum_{k=0}^{K-1} \mathbf{v}_0^T \mathbf{P}^k(\boldsymbol{\lambda}) \mathbf{r}(\boldsymbol{\lambda}) = \boldsymbol{\pi}^T(\boldsymbol{\lambda}) \mathbf{r}(\boldsymbol{\lambda}), \tag{8}$$

where the product $\mathbf{v}_0^T \mathbf{P}^k(\boldsymbol{\lambda})$ indicates the probability distribution of the energy in the tag battery after k time-slots for the transition matrix $\mathbf{P}(\boldsymbol{\lambda})$ defined in (6), $\mathbf{v}_0$ is an arbitrary initial distribution vector, while $\mathbf{r}(\boldsymbol{\lambda}) = [r_{\lambda_0}, ..., r_{\lambda_{N-1}}]^T$ is the read probability vector with entries defined in (7). The right-hand side of (8) follows from the fact that the Markov chain at hand is ergodic (see Sec. IV-A), where $\boldsymbol{\pi}(\boldsymbol{\lambda}) = [\pi_0(\boldsymbol{\lambda}), ..., \pi_{N-1}(\boldsymbol{\lambda})]^T$ is the steady state distribution vector. It also follows that $g(\boldsymbol{\lambda})$ does not depend on the initial vector $\mathbf{v}_0$, but it is uniquely defined by the policy $\boldsymbol{\lambda}$.

The optimal stationary policy $\boldsymbol{\lambda}^* = [\lambda_0^*, ..., \lambda_{N-1}^*]$, is defined as the stationary policy maximizing the long-term average read probability (8), such that: $g(\boldsymbol{\lambda}^*) \geq g(\boldsymbol{\lambda})$, $\forall \boldsymbol{\lambda}$. Notice that the use of stationary policies is not a restriction for the considered system setting (described in Sec. III), as it can be proved that they are optimal for the MDP at hand (see [16]). Notice that, the dependence of (8) on channel statistics and on system parameters is embedded in the definition of $\mathbf{P}(\boldsymbol{\lambda})$ and $\mathbf{r}(\boldsymbol{\lambda})$.

A. Howard Policy Improvement Algorithm

The complexity of a brute force approach algorithm, which exhaustively evaluates all the possible $N!$ policies to find the optimal stationary policy $\boldsymbol{\lambda}^*$, becomes prohibitive for large

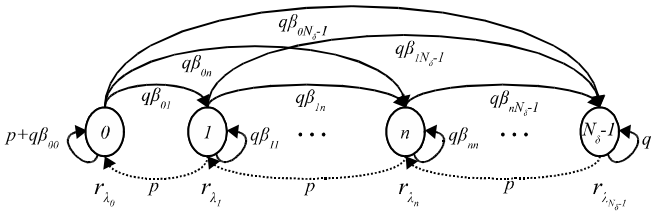

Fig. 3. Markov chain describing the ABEH tag battery state. Dashed lines indicate policy-dependent transitions.

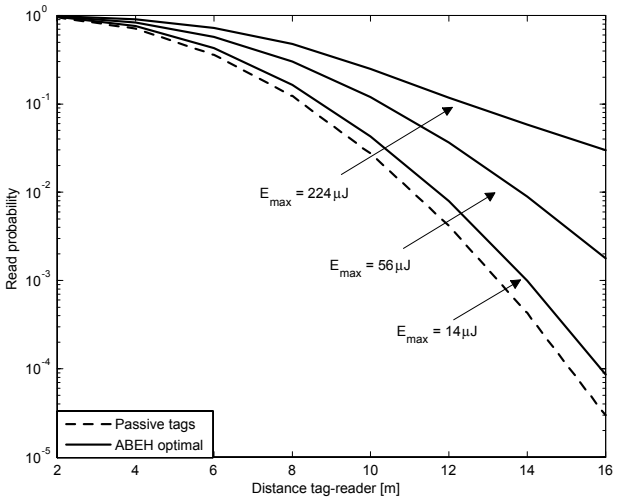

Fig. 4. Long-term average read probability of ABEH and passive tags versus tag-reader distance for different battery sizes ($\gamma_{th}\sigma_r^2 = -67dBm$, $\delta_E = 0.22\,\mu$J, $E_0/T = 36dBm$, $T = 10ms$, $p = 0.1$, $\eta_{amp} = \eta_{\rm mod} = 0.2$, $\eta_{DC} = 0.4$).

N. As alternative approach, we resort to the Howard Policy Improvement Algorithm (HPI-A) [11] that allows the optimal policy to be found in a finite number of steps (generally much lower than the exhaustive search). The starting point for HPI-A is the equation relating the long-term average read probability $g(\boldsymbol{\lambda})$ (8) and the *relative gain vector* $w(\boldsymbol{\lambda}) = [0, w_1(\boldsymbol{\lambda}), ..., w_{N-1}(\boldsymbol{\lambda})]$, whose n-th entry is defined as the gain of having the Markov chain starting in state n rather than in state 0. This vector equation is given by: $\mathbf{w}(\boldsymbol{\lambda}) + g(\boldsymbol{\lambda})\mathbf{1} = \mathbf{r}(\boldsymbol{\lambda}) + \mathbf{P}(\boldsymbol{\lambda})\mathbf{w}(\boldsymbol{\lambda})$, where $\mathbf{1} = [1, ..., 1]^T$ and $\mathbf{P}(\boldsymbol{\lambda})$ is the transition probability matrix defined in Sec. IV-A. Notice that the vector equation above defines a linear system with N equations and N unknowns that are given by $w_1(\boldsymbol{\lambda}), ..., w_{N-1}(\boldsymbol{\lambda})$, since we can arbitrarily fix $w_0(\boldsymbol{\lambda}) = 0$ as reference. The HPI-A is an iterative algorithm converging to the exact solution in a finite number of steps. It works as follows: 1) Choose an arbitrary policy $\boldsymbol{\lambda} = [\lambda_0, ..., \lambda_{N-1}]^T$; 2) Calculate $\mathbf{w}(\boldsymbol{\lambda})$ from the linear system above; 3) If $\mathbf{r}(\boldsymbol{\lambda}) + \mathbf{P}(\boldsymbol{\lambda})\mathbf{w}(\boldsymbol{\lambda}) \geq \mathbf{r}(\boldsymbol{\theta}) + \mathbf{P}(\boldsymbol{\theta})\mathbf{w}(\boldsymbol{\lambda})$ for all possible $\boldsymbol{\theta} = [\theta_0, ..., \theta_{N-1}]^T$ (N entry-wise inequalities have to be satisfied), then $\boldsymbol{\lambda}$ is optimal; 4) Otherwise, find $\boldsymbol{\theta}$ such that at least one of the inequalities above is not satisfied; 5) Update $\boldsymbol{\lambda} = \boldsymbol{\theta}$ and iterate with the new policy steps from 2 to 5 until the algorithm converges (that is, all the N inequalities at step 3 are satisfied). Further details on the HPI-A can be found in [7] and [11].

VI. Numerical Results

We now provide some numerical results to show the read range improvement of ABEH tag with respect to conventional passive tags. We assume DL/UL channels as statistically independent Rayleigh channels. The long-term average read probability (8) of ABEH tags is compared to the one attainable with passive tags, which using the notation above is $g^{std} = \Pr[\gamma(0;k) \geq \gamma_{th}]$ (see [10] for a closed-form expression). We chose δ_E by imposing that $\Pr[\mathcal{E}(k) < \delta_E] \simeq 5\%$ for the maximum distance tag-reader ($d = 16\,$m). This value provides a reasonable trade-off between approximation and complexity of the model. Fig. 4 shows the long-term average read probability versus the tag-reader distance d. Energy-unit is $\delta_E = 0.22\,\mu$J while we vary the size of the battery $E_{\max} \in \{14, 56, 224\}\,\mu$J by changing the size of the discrete model $N \in \{64, 256, 1024\}$ (notice that, keeping δ_E fixed implies more accuracy of the discrete model for distances smaller than $d = 16\,$m, see Sec. IV). The duration of a time-slot is $T = 10\,$ms, the transmitted power is $E_0/T = 36dBm$, while the product between SNR threshold and noise power is $\gamma_{th}\sigma_r^2 = -67dBm$ (this is equivalent to define the power sensitivity of the reader, see (4) for details). The interrogation probability is $p = 0.1$, the CW frequency is $f_0 = 915\,$MHz and the efficiencies are $\eta_{\rm mod} = \eta_{amp} = 0.2$ and $\eta_{DC} = 0.4$. ABEH tags provide considerable gains in terms of read range (for the given requirements $\gamma_{th}\sigma_r^2$) with respect to passive tags, especially for sufficiently large batteries.

We now evaluate the effect of the interrogation probability p and the energy scheduler complexity on the system performance. Low complexity schedulers can discern only $N_L < N$ battery levels, thus needing less memory to store policies ($\boldsymbol{\lambda}$ has N_L elements compared to N) and simpler circuit to measure the battery state. Fig. 5 shows the average read probability of ABEH tags for different values of $N_L \in \{2, 16, 1024\}$ versus p, along with the performance of the draw-all policy for $d = 16m$ and $E_{\max} = 224\,\mu$J (other parameters as above). It is seen that energy schedulers with only $N_L = 16$ states suffers negligible performance penalty with respect to more complex scheduler with $N_L = N$ states. Notice also that, even with $N_L = 2$ states (i.e., a threshold at the half size of the battery), ABEH tags still perform much better than passive tags. Clearly for $p \to 1$ there is no performance gain when using ABEH tags, as no energy can be harvested, while gains of orders of magnitude are possible for smaller p. Finally, the draw-all policy becomes highly suboptimal for moderate-to-high values of p since in this regime, the tag needs to manage accurately the stored energy. The shapes of the policies for a moderate-high interrogation probability $p = 0.1$ versus battery state and for different distances d, are shown in Fig. 6. We notice that, for increasing distances d, the energy scheduling preserves energy until the battery has stored enough energy.

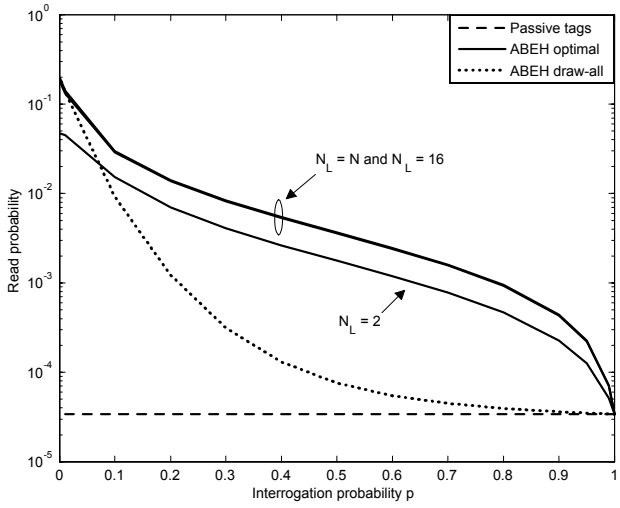

Fig. 5. Long-term average read probability of ABEH and passive tags versus interrogation probability p for different policy complexities N_L ($E_{\max} = 224\,\mu$J, $d = 16m$, other parameters as in Fig. 4).

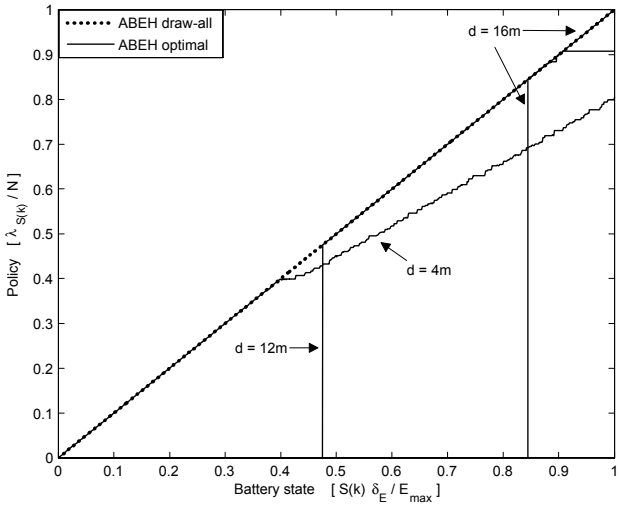

Fig. 6. Normalized policies $\boldsymbol{\lambda}/N$ versus normalized battery state $S(k)\delta_E/E_{\max}$ for different distances tag-reader d ($E_{\max} = 224\,\mu$J, $p = 0.1$, other parameters as in Fig. 4).

VII. Concluding remarks

The problem of increasing the tag read range for passive RFID-based sensor networks limited by the reader sensitivity has been addressed. An approach that leverages an onboard battery at the tag, recharged exclusively through RF-energy harvesting of the reader signal during tag inactivity period, to opportunistically amplify the backscatter signal (Amplified Backscatter through Energy Harvesting, ABEH) has been proposed. The analysis presented in this paper shows remarkable performance gains, in terms of read range, achievable with ABEH tags, even in the presence of moderate-to-large interrogation probabilities, i.e., for a small number of tags and/or high rate of information collection from the tags to reader. Moreover, it points to the importance of a well-designed energy scheduling techniques at the tag, especially in the regime of moderate-to-high interrogation probabilities. Low-complexity policies have also been designed and shown to provide small performance loss over optimal strategies. As a final remark, it is noted that the proposed solution and analysis framework can be extended to the case of tag sensitivity-limited systems, by allowing a trade-off between the use of the on-board battery to amplify the backscatter signal and to reduce the tag sensitivity requirement. Finally, more complex propagation scenario can also be analyzed based on this framework with minor modifications.

References

[1] N. Vaidya and S. R. Das, "RFID-based networks: exploiting diversity and redundancy," Technical Report, University of Illinois at Urbana-Champaign, June 2006.

[2] Klaus Finkenzeller, *RFID Handbook: Fundamentals and Applications in Contactless Smart Cards and Identification, Second Edition*. John Wiley and sons 2003.

[3] P. Nikitin and K. Rao, "Antennas and Propagation in UHF RFID Systems," in *Proc. IEEE RFID conference*, April 2008, Las Vegas, Nevada, USA.

[4] Mays et al., *RFID transponder having active backscatter amplifier for retransmitting a received signal*, United States Patent, Patent No.: US 6,838,989 B1, Jan 2005.

[5] H.C. Liu, M.C. Hua, C.G. Peng, and J.P. Ciou, "A novel battery-assisted class-1 generation-2 RF identification tag design'" *IEEE Trans. Microwave Theory and Techniques*, vol. 57, no. 5, pp. 1388-1397, May 2009.

[6] A. Janek, C. Trummer, C. Steger, R. Weiss, J. Preishuber-Pfluegl, and M. Pistauer, "Lifecycle Extension of Long Range UHF RFID Tags based on Energy Harvesting," in *Proc. EURASIP Workshop on RFID Technology*, Vienna, Austria, Sep. 2007.

[7] J. Lei, R. Yates and L. Greenstein, "A generic model for optimizing single-hop transmission policy of replinishable sensors," *IEEE Trans. Comm.* , vol. 8, no. 2, pp. 547-551, Feb. 2009.

[8] A. P. Sample, D.J. Yeager, P.S. Powledgde, A.V. Mamishev, and J.R. Smith, "Design of an RFID-based battery-free programmable sensing platform," *IEEE Trans. Instrumentations and Measurement*," Vol. 57, no. 11, pp. 2608-2615, Nov. 2008.

[9] A. Janek, C. Trummer, C. Steger, R. Weiss, J. Preishuber-Pfluegl, and M. Pistauer, "Simulation based verification of energy storage architectures for higher class tags supported by energy harvesting devices," in *Proc. 10th Euromicro Conference on Digital System Design Architectures*, Lubeck, Germany, Oct. 2007.

[10] D. Kim, M. A. Ingram, and W. W. Smith, "Measurements of small-scale fading and path loss for long range RF tags", *IEEE Trans. Antennas and Propagation*, vol. 51, no. 8, pp. 1740-1749, Nov. 2003.

[11] R. Gallager, *Discrete stochastic processes*. Kluwer Academic Publisher, 1995.

[12] EPCglobal, "*EPC radio-frequency identity protocols class-1 generation-2 UHF RFID protocol for communications at 860 MHz - 960 MHz version 1.0.9*," EPCglobal Standard Specification, 2004.

[13] G. De Vita and G. lannaccone, "Design criteria for the RF section of UHF and microwave passive RFID transponders," *IEEE Trans. Microwave Theory and Techniques*, vol. 53, no. 9, pp. 2978-2990, Sep. 2005.

[14] J.D. Griffin, G. Durgin, A. Haldi, and B. Kippelen, "Radio link budgets for 915MHz RFID antennas placed on various objects," in *Proc. WCNG Wireless Symposium*, Austin, Texas, Oct. 2005.

[15] D. Panigrahi, S. Dey, R. Rao, K. Lahiri, C. Chiasserini, A. Raghunathan, "Battery life estimation of mobile embedded systems," *in Proc. 14th International Conference on VLSI Design*, Bangalore, India, Jan. 2001.

[16] K.W. Ross, "Randomized and Past-Dependent Policies for Markov Decision Processes with Multiple Constraints," *Operations Research*, vol. 37, no. 3, pp. 474-477, May-Jun. 1989.